51st IEEE Conference on Decision and Control
December 10-13, 2012. Maui, Hawaii, USA

Measuring the degree of modularity in gene regulatory networks from the relaxation of finite perturbations

Kyung Hyuk Kim and Herbert M. Sauro

Abstract— **In gene regulatory networks, transcription factors regulate downstream sites by binding or unbinding to specific promoter regions. It is known that the binding-unbinding process can affect factor life times, and thus response times. This change in the dynamical properties depends on the number of sites that the transcription factor binds to as well as the factor concentration level. To estimate how the dynamics of a given transcription factor will be affected by the number of binding sites, we previously devised a measure called the fan-out – complimentary measure to retroactivity – that indicates the maximum number of the binding sites before the dynamic response is significantly affected. We provided an efficient method to measure the fan-out and retroactivity experimentally by exploiting gene expression noise. In this presentation, we provide another efficient measurement method for retroactivity and fan-out at the population level. The method resorts to finite-size perturbations in system parameters or concentrations. The equivalent analysis method at the single cell level that is based on gene expression noise is also presented.**

I. INTRODUCTION

Synthetic biology aims to engineer biological organisms with new functionalities by designing and constructing regulatory systems – synthetic circuits – from smaller network components. This bottom-up approach benefits from modularity [1], [2], [3], [4], [5], [6], [7]. The input and output of the circuit components are commonly considered the concentration levels of regulatory proteins, e.g., transcription factors in gene regulatory networks and proteins in signal transduction networks. In this presentation, we limit modularity with respect to the functional relationship between the input-output (i/o) of circuit components.

In biological reaction networks, regulation is often achieved by sequestration which in turn changes the response time of the network [8], [9]. When two networks, or modules, are connected via a sequestration mechanism, the change in response times can affect the dynamics of the upstream module. This effect is called retroactivity [10], [11].

The more the retroactivity, the less modular the network. Thus, it is desirable to reduce the retroactivity for modular construction of biological networks. To quantify this retroactivity, we proposed operational methods for measuring the retroactivity in the stochastic framework [11]. For example, in gene regulatory networks, gene expression noise [12], [13], [14], [15] observed at the single cell level can be leveraged to quantify the response time [11]. The noise – protein concentration fluctuations in time – can be considered as a response to continuous perturbations appearing in the system due to random biological reactions. Thus, from the noise one can obtain the system's dynamical information including the response time, without applying laborious system perturbations. Specifically, experiments for this measurement can be performed by obtaining fluorescence signals from multiple single cells at different time points that are tracked via a fluorescence microscope, and by computing the temporal signal-correlations. One of the downsides of this approach is the limited sample size for computing the response time.

The response time can be also measured at the population [9] level. This approach requires perturbations in the system and the observations of its relaxation dynamics. The disadvantage of this approach is to maintain the exponential growth of cells sufficiently long enough to observe the relaxation. This can be overcome by introducing continuous culture through a chemostat. The down-side in both the single-cell and population-level approaches have hampered experimental measurement of the retroactivity *in vivo*, although retroactivity has been observed in signal transduction networks *in vitro* [9], [8]. The systematic and less-error-prone measurement method for retroactivity, especially suited for gene regulatory networks, is still lacking at the population level, although the operational method at the single-cell level exists.

Fan-out is a complimentary measure to retroactivity that indicates how much of a 'load' an upstream network can regulate. The fan-out was shown to be efficiently characterized by using a certain linear relationship between the response time of the transcription factor and the downstream load [16]. This linearity was shown to be valid for a wide class of module interfaces (Fig. 1) [16]. The linearity has not been confirmed by experiment for any biological networks yet, because of the same issues related to retroactivity measurements.

Here we will leverage this linearity to measure the retroactivity and fan-out with a higher accuracy at the population level, and discuss how to design single-cell and population level experiments and which biological quantities need to be measured to observe the linearity.

II. FAN-OUT AND RETROACTIVITY: REVIEW

Consider a module interface process (MIP) shown in Fig. 1. This MIP can be mathematically expressed as a set

Kyung Hyuk Kim is Acting Assistant Professor of the Department of Bioengineering, University of Washington, William H. Foege Building, Box 355061, Seattle, WA 98195-5061, USA kkim@uw.edu

Herbert M. Sauro is Associate Professor of the Department of Bioengineering, University of Washington, William H. Foege Building, Box 355061, Seattle, WA 98195-5061, USA hsauro@u.washington.edu

978-1-4673-2066-5/12/$31.00 ©2012 IEEE

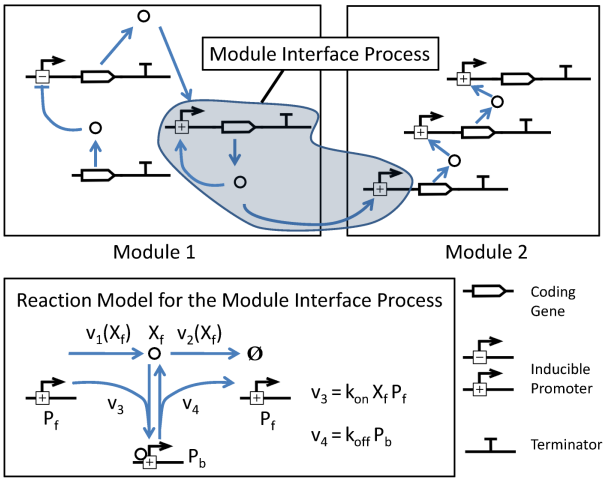

Fig. 1: Module interface process between Modules 1 and 2

of ordinary differential equations:

$$\frac{dX_f}{dt} = v_1(X_f) - v_2(X_f) - k_{\text{on}}X_f P_f + k_{\text{off}}P_b, \quad (1)$$

$$\frac{dP_b}{dt} = k_{\text{on}}X_f P_f - k_{\text{off}}P_b, \quad (2)$$

where X_f denotes the concentration of the free TF, P_f that of the specific promoter that is not bound by the TF, and P_b that of the bound promoter. Note that the transcription factor can bind and unbind to the promoter region and thus Module 2 can affect the properties of Module 1. v_1 denotes the synthesis rate of the TF with its autoregulation and v_2 denotes the degradation that could include first-order reaction and enzyme-mediated reactions (when the TF is tagged for degradation) such as Michaelis-Menten kinetics. We assume that the TF binding-unbinding reactions are fast enough that P_b is in quasi-equilibrium. Therefore, the concentration of the bound TF will be determined by the equilibration of the fast reactions:

$$k_{\text{on}}X_f P_f = k_{\text{off}}P_b. \quad (3)$$

However, there are slow dynamics due to the synthesis and degradation processes (v_1 and v_2). These slow reactions affect the change in the concentration levels of both the free and bound TFs. More specifically, the *total* TF changes due to these slow reactions. Mathematically, by summing both (1) and (2), we obtain

$$\frac{dX_T}{dt} = v_1(X_f) - v_2(X_f), \quad (4)$$

where $X_T \equiv X_f + P_b$, denoting the total TF concentration. By substituting $P_b = X_T - X_f$ to (3), X_T can be expressed in terms of X_f, i.e., mathematically $X_T(X_f(t))$, and this expression can be substituted to (4), resulting in the following equation:

$$(1 + \mathcal{R}(X_f))\frac{dX_f}{dt} = v_1(X_f) - v_2(X_f), \quad (5)$$

where

$$\mathcal{R}(X_f) \equiv \frac{dX_T}{dX_f} - 1 = \left(1 + \frac{X_f}{K_d}\right)^{-2}\frac{P_t}{K_d}, \quad (6)$$

with K_d the dissociation constant for the TF binding-unbinding reactions, equal to $k_{\text{off}}/k_{\text{on}}$, and P_t the total number of the downstream promoters including bound and free promoters: $P_t = P_b + P_f$. The extra factor $1 + \mathcal{R}$, appearing in front of dX_f/dt, has a mechanistic meaning that the speed of the change in X_f is stretched out by $1+\mathcal{R}$: If $\mathcal{R}$ is positive, the dynamics slows down due to the TF binding-unbinding reactions and if negative, it speeds up. This is the effect from the downstream, which is called retroactivity [10]. Here, the degree of retroactivity will be quantified by $\mathcal{R}$, in a rather different way than the original definition [10], since this new way of definition [17] is more straightforward in its biological interpretation.

The retroactivity $\mathcal{R}$, defined in (6), shows an interesting property that it increases in proportional to the total number of promoters including the bound and free forms [16]. This linearity was shown to be valid for a wide class of MIPs and to play an important role in making connections between retroactivity and fan-out [16], where the fan-out defines the maximum number of the downstream promoters that can be driven by the upstream TF. By leveraging the linearity, fan-out was shown to be efficiently estimated by performing a minimal number of experiments.

One caveat in the expression of the retroactivity Eq. (6) is that $\mathcal{R}$ can be significantly dependent on the concentration level, X_f, relative to K_d. This dissociation constant has a biological meaning that when X_f is equal to the dissociation constant K_d, half of the promoters are found bound. Thus, the retroactivity can increase significantly when $X_f < K_d$, i.e., when P_b is comparable to X_f. This indicates that characterization of module interface processes is significantly dependent on the state of the processes, i.e., X_f. Here we provide operational methods that can efficiently measure the average retroactivity over the state variation.

III. Theoretical Results

A. Measuring the degree of modularity under finite-size perturbations

This section describes an efficient way of measuring retroactivity at the population-level. Consider that at a certain time point ($t = 0$), the system is perturbed from a stationary state, for example, by increasing the synthesis rate v_1 or blocking the degradation rate v_2. Under such perturbations, the concentration level X_f will move from one stationary state to another. Here we assume that the change is monotonic. Then, (5) can be expressed as follows:

$$\mathcal{R}(X_f) = \frac{dt}{dX_f}(v_1(X_f) - v_2(X_f)) - 1,$$

where $\frac{dt}{dX_f}$ indicates the change in the response time due to the change in X_f. This equation means that the retroactivity can be measured by observing the slope (more precisely its inverse) in the transient response in X_f, as it approaches to a new stationary state. The extra factor $v_1 - v_2$ can be measured by observing the transient response without any

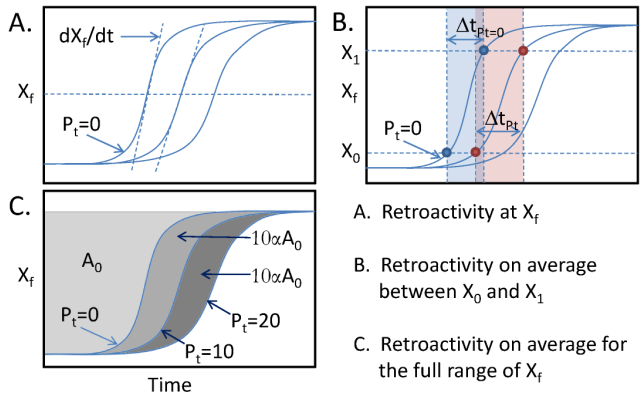

Fig. 2: Operational methods for measuring retroactivity based on perturbation experiments: (A) The ratios of the slopes indicated by dotted lines can be used for estimating retroactivity: Eq. (7). (B) The ratios of the time intervals (Δt) (blue and red) is directly related to retroactivity on average for the range of X_f (the area between the two horizontal dotted lines): Eq. (8). (C) The ratios of the areas can be used for retroactivity on average for the whole response range of X_f: Eq. (10). $\mathcal{R}$ is equal to, for example, 10α for $P_t = 10$ and 20α for $P_t = 20$.

downstream connection:

$$\frac{dX_f}{dt} = v_1(X_f) - v_2(X_f).$$

Therefore, the retroactivity can be estimated by comparing the two slopes for the connected and isolated case, for a given value of X_f:

$$\mathcal{R}(X_f) = \frac{(dt/dX_f)_{P_t}}{(dt/dX_f)_{P_t=0}} - 1. \tag{7}$$

As shown in Fig. 2A, by comparing the two different transient response curves corresponding to the connected and isolated cases, respectively, one can obtain the retroactivity for a given X_f that was reached due to the perturbation.

If the time profile of $X_f(t)$ is noisy and thus retroactivity cannot be estimated accurately, a range of the concentration levels – not a single point – can be used. The above equation can be approximately expressed:

$$\mathcal{R}(X_f) \simeq \frac{\Delta t_{X_0 \to X_1; P_t}}{\Delta t_{X_0 \to X_1; P_t=0}} - 1. \tag{8}$$

By measuring the time durations for a given response signal change ($X_0 \to X_1$) for both the connected and isolated cases, the retroactivity can be estimated in the average sense for the range of the concentration level $X_0 < X_f < X_1$ (Fig. 2B).

If the time profile of $X_f(t)$ is even noisier – which can often be the case in real experiments – the range of the concentration level needs to be extended to the full range of the concentration from one stationary state value to another corresponding to before and after the perturbation. In this case, the retroactivity can be measured in a rather different way than (8), which will be described in the next section.

B. Measuring the degree of modularity from the full response curves

One interesting fact in the time-response curve is that it shows a linear relationship between the response time to reach a certain concentration level (X_f) and the number of promoters. This linear relationship was theoretically studied in [9] for a particular signal transduction network for the case of finite-size perturbations. This relationship was also investigated in our previous fan-out study in both the deterministic and stochastic regimes [16]. We generalize this result to a wider class of module interface processes that were investigated in our previous fan-out study [16].

Consider the response time for X_f to reach a particular concentration level (X^*) from X_0, by rearranging (5):

$$\frac{1 + \mathcal{R}(X_f)}{v_1(X_f) - v_2(X_f)} dX_f = dt.$$

The time taken to reach X^* will be denoted by t^* (we assumed here that perturbation is applied at $t = 0$), which can be computed as follows:

$$t^* = \int_{X_0}^{X^*} dX_f \frac{1 + \mathcal{R}(X_f)}{v_1(X_f) - v_2(X_f)}$$

Let us introduce one measurable quantity, the area of response A_{P_t}, which corresponds to the sum of t^* for the full range of response in X_f, as described in Fig. 2C, which can be computed by integrating t^* over $X_0 < X_f < X_1$:

$$\begin{aligned} A_{P_t} &= \int_{X_0}^{X_1} dX' \int_{X_0}^{X'} dX_f \frac{1 + \mathcal{R}(X_f)}{v_1(X_f) - v_2(X_f)} \\ &\simeq (1 + \tilde{\mathcal{R}}) \int_{X_0}^{X_1} dX' \int_{X_0}^{X'} dX_f \frac{1}{v_1(X_f) - v_2(X_f)} \\ &= (1 + \tilde{\mathcal{R}}) A_0, \end{aligned} \tag{9}$$

where $\tilde{R}$ can be considered the retroactivity for the full response range in X_f. By rearranging the terms in the above equation, we obtain

$$\tilde{\mathcal{R}} = \frac{A_{P_t} - A_0}{A_0}. \tag{10}$$

This indicates that from the area ratio, the retroactivity for the full response can be computed from the response curves and their difference in their whole profiles (Fig. 2C).

By using the fact that $\mathcal{R}$ increases linearly with P_t (refer to (6) for the simple MIP (Fig. 1) and the results in the Appendix of [16] for more general MIPs):

$$\mathcal{R} \equiv \alpha(X_f) P_t,$$

we obtain the response time difference between the connected and isolated cases:

$$t^*_{P_t} - t^*_{P_t=0} = P_t \int_{X_0}^{X^*} \frac{\alpha(X_f)}{v_1(X_f) - v_2(X_f)} dX_f, \tag{11}$$

indicating that the response time difference is proportional to the number of P_t. This fact indicates that one can construct response curves for the case of arbitrary number of promoters, once two different response curves are known

corresponding to different values of P_t. Thus, if the linear relationship is valid in real experimental conditions, this linearity will lead to fast prediction on how the system responds under the different numbers of promoters and eventually will expedite the characterization of fan-out values corresponding to a range of responses in X_f.

Furthermore, the linear relationship (11) can significantly increase the accuracy of fan-out measurements. Here without taking the approximation step performed after (9), equation (11) was derived. This equation indicates that the difference in the two areas of response $A_{P_t} - A_{P_t'}$ is linearly related to $P_t - P_t'$. Specifically, (9) can be used to obtain

$$A_{P_t} = A_0 + \beta P_t, \tag{12}$$

where

$$\beta \equiv \int_{X_0}^{X_1} dX' \int_{X_0}^{X'} dX_f \frac{\alpha(X_f)}{v_1(X_f) - v_2(X_f)}.$$

Here, A_{P_t} is a less error-prone quantity, compared to a response time difference $t^*_{P_t} - t^*_{P_t=0}$ (since A is the sum of the response time). Thus, experimental verification of the linear relationship can be performed efficiently in this way.

Retroactivity can be measured by substituting (12) to (10), resulting in

$$\boxed{\mathcal{R} = \beta P_t / A_0}. \tag{13}$$

Fan-out can be also measured from (11) and (12). The average response time for the full response curve can be expressed, by dividing (12) by $X_1 - X_0$:

$$\overline{t^*_{P_t}} = \overline{t^*_{P_t=0}} + \frac{\beta}{X_1 - X_0} P_t.$$

If the desired maximum response time for Module 1 is T_{M1}, the average response time of the transcription factor, $\overline{t^*_{P_t}}$, needs to be controlled below T_{M1}:

$$\overline{t^*_{P_t=0}} + \frac{\beta}{X_1 - X_0} P_t < T_{\text{M1}}.$$

Therefore, we obtain the fan-out (on average):

$$\boxed{F = \text{MAX}(P_t) = \frac{(T_{\text{M1}} - \overline{t^*_{P_t=0}})(X_1 - X_0)}{\beta}}, \tag{14}$$

where T_{M1} is provided by the desired property of Module 1, $\overline{t^*_{P_t=0}}$ can be computed by $A_0/(X_1 - X_0)$, and β by the slope in the graph of A_{P_t} vs. P_t (refer to (12)).

C. Information on retroactivity from gene expression noise

Let us consider that the transcription factor is tagged for fluorescence. The fluorescence signal can be observed at the single cell level, and its time course can be measured via fluorescence microscopy. The signal fluctuations in time can be considered as the outcome of random biological reactions such as transcription, translation, and cell growth. These sources of noise are often classified into intrinsic and extrinsic noise depending on whether the biological reactions serving as noise sources can be included as systems of interest or not. The intrinsic noise is often considered a fast-fluctuating signal (small correlation time) compared to the extrinsic noise, although there are potential problematic issues in how to separate the two different noise types in the fluorescence signals: The system that generates the extrinsic noise can also involve other transcription and translation processes and the noise generated from there can also be fast-fluctuating and propagated to the system of interest.

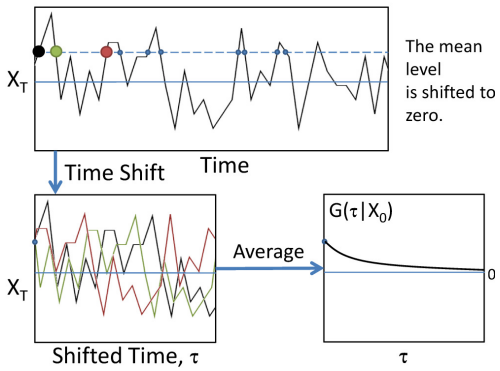

Fig. 3: Population level dynamics obtained from gene expression noise at the single cell level

For mathematical simplicity, we assume that the dynamics of the system of interest is much faster than that of the surroundings, i.e., the intrinsic noise fluctuates much faster than the extrinsic noise and the extrinsic noise is neglected (refer to [11] for the case when taking into account the extrinsic noise). From the previous master equation approach [16], [11], we investigated how to relate retroactivity to gene expression noise by using autocorrelation functions, and found that the correlation time in the fluorescence signal is directly related to the response time measured at the population level. This stochastic fan-out and retroactivity quantities were shown to be well matched with their corresponding deterministic ones for realistic parameters for experiments.

Here we propose a different measurement quantity obtained from the fluorescence signals to directly visualize the transient response that could be observed at the population level. The quantity is the conditional expectation value of the fluorescence signals (X_T) measured with a time lag τ when the signal value was given as $X_T = X_0$ at $\tau = 0$ (Fig. 3):

$$G(\tau|X_0) \equiv E[X_T(t = t_0 + \tau)|X_0] - E[X_T], \tag{15}$$

where $G(\infty|X_0)$ converges to 0 since the initial value of X_0 would not affect X_T for sufficiently large time lags. This quantity serves as the time trajectory of the average value of X_T for the initial probability distribution corresponding to $X_T = X_0$ (ergodicity is assumed). Therefore, gene expression noise can be leveraged to realize the finite size perturbation experiments (not in the system parameters, but in the concentration levels). The same methods as presented in the previous sections to measure retroactivity at the population level can be used for this single-cell level experiments.

Stochastic and deterministic simulations performed for the MIP shown in Fig. 1. $G(\tau|X_0)$ matched well with the deterministic results (Fig. 4A). For the deterministic case,

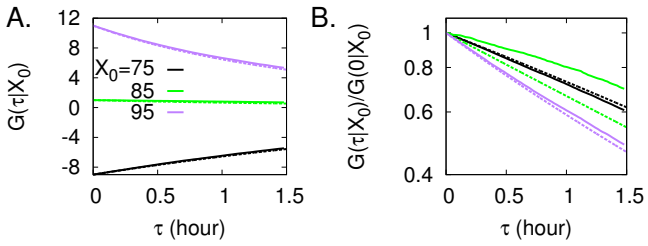

Fig. 4: $G(\tau|X_0)$ for the MIP shown in Fig. 1. Parameters: $v_1 = 8$ nM/h, $v_2 = \gamma X_f$ with $\gamma = 2$ h^{-1}, $k_{\text{on}} = 10$ h^{-1}nM^{-1}, $k_{\text{off}} = 10$ h^{-1}. We interchanged the unit of nM and copy number.

the initial values of X_f and P_b were set to the equilibrium values in the binding-unbinding processes for a given value of $X_T = X_0$, by using (3). $G(\tau|X_0)$ was shown to decay with a different characteristic time for a different value of X_0 and the speeds of relaxation, i.e., the characteristic times of decay (the inverse slope in the figure), were well matched with the deterministic cases (Fig. 4B) except for the cases where X_0 is close to the mean value (probably, due to discreteness in copy numbers). Since the characteristic time is related to the retroactivity, this result indicates that the retroactivity values obtained from gene expression noise data will well match those for the deterministic cases.

IV. Numerical Example

This section presents a MIP that includes a negative feedback and dimerization and explicit mRNA processes as shown in Fig. 5. This process can be mathematically described by

$$\begin{aligned}
\dot{S}_1 &= v_1 - v_2 \\
\dot{S}_2 &= v_3 - v_4 - 2v_5 + 2v_6 \\
\dot{S}_3 &= v_5 - v_6 - v_7 - v_8 + v_9 - v_{10} + v_{11} \\
\dot{S}_4 &= v_8 - v_9 \\
\dot{S}_5 &= -v_8 + v_9 \\
\dot{S}_6 &= v_{10} - v_{11} \\
\dot{S}_7 &= -v_{10} + v_{11},
\end{aligned} \tag{16}$$

where

$$\begin{aligned}
v_1 &= k_1 S_7 & v_2 &= k_2 S_1 & v_3 &= k_3 S_1 \\
v_4 &= k_4 S_2 & v_5 &= k_5 S_2(S_2 - 1) & v_6 &= k_6 S_3 \\
v_7 &= k_7 S_3 & v_8 &= k_8 S_3 S_5 & v_9 &= k_9 S_4 \\
v_{10} &= k_{10} S_3 S_7 & v_{11} &= k_{11} S_6.
\end{aligned}$$

We compared the retroactivity measured by using the stochastic and deterministic models. For the deterministic model, (16) was used and finite perturbations corresponding to a decrease in the negative feedback were applied by increasing the rate of k_{11}. For the stochastic experiments, the Gillespie simulation algorithm [18] was used and only the intrinsic noise (generated from the listed reactions $v_1 \cdots v_{11}$) was considered.

We observed the transient response of the system under the perturbations described above. The concentration level of

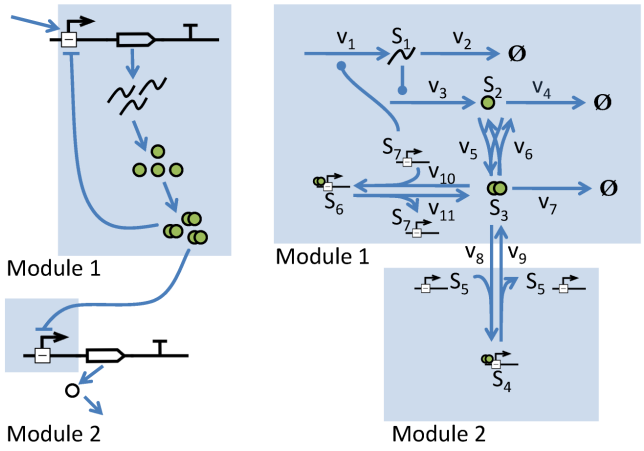

Fig. 5: Module interface process where a dimer inhibits the expression of both the downstream (Module 2) and the upstream (Module 1) promoter expression. S_1 denotes mRNA transcribed from the "output" gene in Module 1, S_2 its monomer unit of the dimer transcription factor S_3, S_4 and S_5 (S_6 and S_7) the Module 2 (Module 1) promoter region when bound and unbound, respectively.

the free transcription factor, S_2, was shown to overshoot and then relax to its new stationary state value (Fig. 6A). The overshoot is related to the time-delayed negative feedback. Once k_{11} is increased, the mRNA (S_1) builds up quickly and overshoots (in the time scale of $\sim$ 2 min) and leads to the translation of the transcription factor (S_2), which responds slowly (in the time scale of $\sim$ 30 min). After the transcription factor binding-unbinding to the promoter regions, the negative feedback suppresses the overshoot amount of S_1 and S_2. Due to this non-monotonic behavior as well as the mixture of the slow and fast time scale fluctuations (due to the binding-unbinding processes) [11], [16], we decided to use a different measurement quantity, the total concentration level of the transcription factor (in the monomer unit), $X_T = S_2 + 2(S_3 + S_4 + S_6)$ [16], [11].

X_T was used for comparing $\mathcal{R}$ for different P_t. Its transient response was shown to be monotonic over time (the overshoot in S_2 due to the overshoot in S_1 was compensated by S_6) (Fig. 6A). The level of X_T before perturbation (at the stationary state), however, was dependent on P_t and we offset them to zero (Fig. 6B). The full change in X_T after perturbation was also dependent on P_t and we rescaled them to 1 (Fig. 6B). Retroactivity, estimated by using the slope-ratio (7), was shown to change with the value of X_T (Fig. 6C) and the area of response A to increase linearly for different number of the downstream promoters P_t (Fig. 6C and D). This confirms the linearity in the response time and the downstream number of promoters, implying a possibility for the efficient characterization of fan-out [16].

Stochastic simulations were performed to confirm that the transient response at the population level can be obtained from gene expression noise. The conditional expectation value, $G(\tau|X_0)$ obtained from the gene expression noise

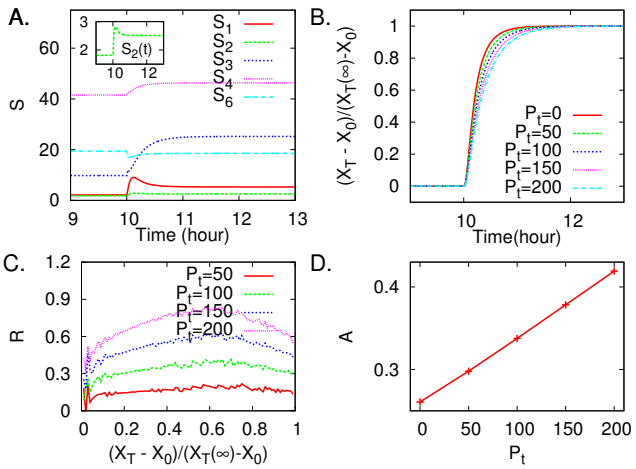

Fig. 6: Retroactivity measurement under finite perturbations: The model described in Fig. 5 was deterministically simulated by using (16). (A) A finite perturbation in the system parameter k_{11} was applied at $t = 10$h. (B) Normalized response in the total transcription factor number in monomer unit was shown to be affected by the downstream load change, P_t. (C) Retroactivity depends on X_T and linearly increases with P_t and (D) this linearity was observed more clearly by computing the area of response. Unit: nM for S and X_T. Parameters: $k_1 = 72\text{h}^{-1}$, $k_2 = 20\text{h}^{-1}$, $k_3 = 20\text{h}^{-1}$, $k_4 = 2\text{h}^{-1}$, $k_5 = 20\text{h}^{-1}\text{nM}^{-1}$, $k_6 = 1\text{h}^{-1}$, $k_7 = 2\text{h}^{-1}$, $k_8 = 10\text{h}^{-1}\text{nM}^{-1}$, $k_9 = 20\text{h}^{-1}$, $k_{10} = 10\text{h}^{-1}\text{nM}^{-1}$, $k_{11} = 3$ and 20h^{-1} before and after the perturbations, respectively.

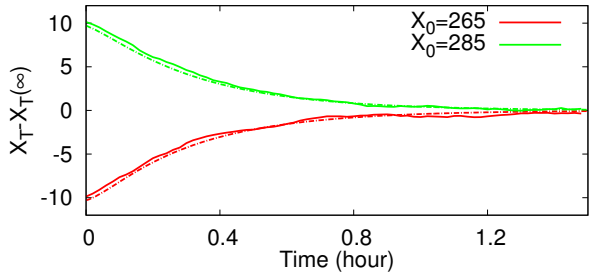

Fig. 7: $G(\tau|X_0)$ vs. time trajectories obtained from the deterministic model: The trajectories (dotted lines) were obtained from (16) and $G(\tau|X_0)$ (solid lines) were obtained by using the Gillespie stochastic algorithm [18]. Parameters: refer to Fig. 6 caption, $k_{11} = 20\text{h}^{-1}$.

matched well with the transient response based on the deterministic model (Fig. 7).

Retroactivity and fan-out estimation: Retroactivity and fan-out (on average) for the full response was estimated by using (13) and (14). A_0 is the response area after the perturbation is applied ($t = 10$hr in Fig. 6). $X_1 - X_0$ is one. β is the slope in Fig. 6D. Then, we obtain $\mathcal{R} = 0.003 \times P_t$ and $F = (T_{\text{M1}} - 0.26)/0.00079$. For $T_{\text{M1}} = 0.5$ hr, F is equal to 300, i.e., the maximum number of the downstream TF specific binding sites are 300 for the desired response time, 0.5 hr.

V. CONCLUSIONS

We investigated fan-out and retroactivity in both the deterministic and stochastic regimes and provided less error prone operational methods for measuring them. The deterministic approach was based on finite-size perturbations and the stochastic one on gene expression noise. The proposed approach was used to confirm the linear relationship between the response time of transcription factors and the number of their specific downstream promoters. Our approach will expedite the characterization of module interfaces of synthetic gene circuit components by quantifying fan-out and retroactivity, at both the single-cell and population levels. Eventually it will provide a step toward for modular construction of synthetic circuits.

VI. ACKNOWLEDGMENTS

The authors gratefully acknowledge the contribution of NSF (No. 0827592 in Theoretical Biology, No. 1158573 in Molecular and Cellular Biosciences).

REFERENCES

[1] P. E. M. Purnick and R. Weiss, "The second wave of synthetic biology: from modules to systems.," *Nat. Rev. Mol. Cell Biol.*, vol. 10, pp. 410–422, June 2009.
[2] J. B. Lucks, L. Qi, W. R. Whitaker, and A. P. Arkin, "Toward scalable parts families for predictable design of biological circuits," *Curr. Opin. Microbiol.*, vol. 11, no. 6, pp. 567–573, 2008.
[3] J. D. Keasling, "Synthetic biology for synthetic chemistry.," *ACS Chem. Biol.*, vol. 3, pp. 64–76, Jan. 2008.
[4] R. Entus, B. Aufderheide, and H. M. Sauro, "Design and implementation of three incoherent feed-forward motif based biological concentration sensors.," *Syst. Synth. Biol.*, vol. 1, pp. 119–128, 2007.
[5] C. A. Voigt, "Genetic parts to program bacteria.," *Curr. Opin. Biotechnol.*, vol. 17, pp. 548–557, Oct. 2006.
[6] D. Sprinzak and M. B. Elowitz, "Reconstruction of genetic circuits.," *Nature*, vol. 438, pp. 443–448, Nov. 2005.
[7] D. Endy, "Foundations for engineering biology.," *Nature*, vol. 438, pp. 449–453, Nov. 2005.
[8] A. C. Ventura, P. Jiang, L. Van Wassenhove, D. Del Vecchio, S. D. Merajver, and A. J. Ninfa, "Signaling properties of a covalent modification cycle are altered by a downstream target," *Proc. Natl. Acad. Sci. U. S. A.*, vol. 107, pp. 10032–10037, 2010.
[9] P. Jiang, A. C. Ventura, E. D. Sontag, S. D. Merajver, A. J. Ninfa, and D. Del Vecchio, "Load-induced modulation of signal transduction networks.," *Science Signaling*, vol. 4, p. ra67, Jan. 2011.
[10] D. Del Vecchio, A. J. Ninfa, and E. D. Sontag, "Modular cell biology: retroactivity and insulation.," *Mol. Syst. Biol.*, vol. 4, p. 161, 2008.
[11] K. H. Kim and H. M. Sauro, "Measuring retroactivity from noise in gene regulatory networks.," *Biophys. J.*, vol. 100, pp. 1167–1177, Mar. 2011.
[12] C. V. Rao, D. M. Wolf, and A. P. Arkin, "Control, exploitation and tolerance of intracellular noise.," *Nature*, vol. 420, pp. 231–237, Nov. 2002.
[13] J. M. Raser and E. K. O'Shea, "Control of stochasticity in eukaryotic gene expression.," *Science*, vol. 304, pp. 1811–1814, June 2004.
[14] M. Kæ rn, T. C. Elston, W. J. Blake, and J. J. Collins, "Stochasticity in gene expression: from theories to phenotypes.," *Nat. Rev. Genet.*, vol. 6, pp. 451–464, June 2005.
[15] V. Shahrezaei, J. F. Ollivier, and P. S. Swain, "Colored extrinsic fluctuations and stochastic gene expression.," *Mol. Syst. Biol.*, vol. 4, p. 196, 2008.
[16] K. H. Kim and H. M. Sauro, "Fan-out in Gene Regulatory Networks.," *J. Biol. Eng.*, vol. 4, p. 16, Dec. 2010.
[17] S. Jayanthi and D. Del Vecchio, "On the Compromise between Retroactivity Attenuation and Noise Amplification in Gene Regulatory Networks.," *Proc. IEEE Conf. Dec. Control*, pp. 4565–4571, 2009.
[18] D. T. Gillespie, "Exact stochastic simulation of coupled chemical reactions.," *J. Phys. Chem.*, vol. 81, pp. 2340–2361, 1977.